Pressure−Volume−Temperature Dependence of Polypropylene/ Organoclay Nanocomposites

L. A. Utracki*,† and R. Simha‡

National Research Council Canada, Industrial Materials Institute, 75 de Mortagne, Boucherville, QC, Canada J4B 6Y4, and Department Macromolecular Science and Engineering, Case Western Reserve University, Cleveland, Ohio 44106-7202

Received August 24, 2004; Revised Manuscript Received October 7, 2004

ABSTRACT: The pressure−volume−temperature (*PVT*) dependencies of commercial polypropylene melt (PP) and its nanocomposites containing X wt % of organoclay (Cloisite-15A, or C15) and $2X$ wt % of a compatibilizer were determined at $T = 450-530$ K and $P = 0.1-190$ MPa. C15 was used at concentrations: $X = 0$, 2, and 4 wt %. Three functionalized PP's were used as compatibilizers: two maleated and one grafted with glycidyl methacrylate. Incorporation of $X = 2$ wt % C15 into PP resulted in reduction of specific volume by $\Delta V \approx 1\%$, but that of free volume (hole) fraction by $\Delta h \approx 5\%$. The latter quantity was computed from the Simha−Somcynsky lattice−hole equation of state. Furthermore, at constant T and P the hole fraction was found to be linearly related to the bulk-average energetic interaction parameter and to be a sensitive indicator of structural changes. In binary (polymer + organoclay) systems Δh is linearly related to the interlayer spacing, d_{001}. So, where statements from the previous paper are repeated or there are similarities, this is done for purposes of comparison. In three-component systems (with a compatibilizer) the proportionality has been preserved, but large changes of Δh result in relatively small changes of d_{001}. Mechanical properties hardly correlate with either Δh or d_{001}, as polymer/ compatibilizer morphology and crystallinity complicate the behavior.

I. Introduction

The pressure−volume−temperature (*PVT*) dependencies of polymers have been measured mainly to determine compressibility and the thermal expansion coefficient. The dependence is a reflection of the internal structure and the volume-averaged interactions, which can be calculated if the experimental data are precise enough and good theoretical description is available. Rodgers published a comprehensive review of six better-known equations of state (eos's) used for polymeric liquids.[1] Recently,[2] the *PVT* behavior of polyamide-6 (PA-6)-based nanocomposites was analyzed using Simha−Somcynsky (S−S) eos.[3] The theory provided an important insight into interactions and structure as well as information on the free volume content given by the hole fraction, h.

Rigorous analyses of the polymeric nanocomposite (PNC) behavior are relatively recent.[4] The first *PVT* studies on PNC with poly-ϵ-caprolactam (PA-6) as the matrix[2] showed that the experimental data for the polymer and its PNC follow the S−S eos with similar accuracy. The fitting yielded the *PVT* reducing parameters (P^*, T^*, and V^*) related to the two Lennard-Jones parameters: the maximum attractive energy, ϵ^*, and the corresponding segmental repulsion volume, v^*. For single-component polymeric liquids the *PVT* behavior is fully described by these two parameters through the eos.

For binary systems containing substances 1 and 2, a random distribution of statistical segments of the two components has been assumed; thus, six parameters need to be determined (11, 12, and 22; for ϵ^* and v^*).[5] This approach has been successful in describing miscible polymer blends, e.g., polystyrene (PS) with poly(phenylene ether) (PPE).[6] However, for PNC such a mean-average model was found inadequate.[2] The inadequacy consists of treating the composite as a simple random mixture of filler and neat polymer, with the latter having fixed 11 parameters. The failure originates in the well-known adsorption on the high-energy surface of crystalline montmorillonite (MMT) platelets. For example, Israelachvili et al.[7] and Horn and Israelachvili[8] used the surface force analyzer (SFA) to measure the viscosity of PS solutions. The authors reported a solidlike behavior for the first 2−9 nm thick surface layer and then a progressive decrease of viscosity with distance from the platelet. Only 100−120 nm away from the crystalline solid was the average bulk solution viscosity obtained. More recently, Luengo et al. used redesigned SFA to measure nanorheological responses of undiluted polybutadiene (PBD).[9] The measurements indicated the presence of an incompressible "hard wall" at $z_{hw} \cong 5$ nm formed by a solidlike PBD adsorbed on the mica surface and a roughly exponential decay at larger distances. Similar behavior has been observed in numerical "experiments" using molecular modeling.[10,11]

In consequence, to interpret the concentration-dependent variations of the binary interaction parameters in PNC, the following model was adopted: the flat MMT plates of specified diameter are covered with an uniform layer of solidified polymer of specified thickness, above which the matrix polymer molecules diffuse into the molten matrix. The segmental mobility of these "hairy" clay platelet (HCP) macromolecules increases with the distance from the clay surface in the normal direction, at an upper limit reaching the neat matrix values. Thus, the characteristic interaction parameters of the matrix vary with the interparticle distance and hence with clay content.

While the manufacture of polyamide (PA)-based PNC is relatively simple,[12] that based on polyolefins (PO) is most difficult. The reason is the apolar character of PO

† National Research Council Canada.
‡ Case Western Reserve University.

10.1021/ma048262z CCC: $27.50
Published on Web 11/24/2004

Table 1. Polymers Used in This Study[a]

code	type	trade name	M_w (kg/mol)	composition	manufacturer
PP[b]	polypropylene	SM 6100	264	neat homopolymer	Montell
E43	PP-*g*-MAH	Epolene-43	9.1	9.79% MAH	Eastman
315	PP-*g*-MAH	Polybond−3150	330	1.0% MAH (ST present)	Uniroyal
GMA	PP-*g*-GMA		305	0.42% GMA (ST present)	NRCC/IMI[37]

[a] Notes: PP-*g*-MA or PP-*g*-GMA is polypropylene grafted respectively with maleic anhydride (MAH) or glycidyl methacrylate (GMA); to increase the grafting efficiency styrene (ST) is often used. [b] The melt flow rate of PP, MFR = 11 deg/min.

macromolecules and general immiscibility even within the same chemical family (e.g., LDPE being immiscible with most LLDPE's).[13] In principle, clay preintercalated with end-terminated PO macromolecules should yield exfoliated PNC, provided that the matrix resin has the same chain composition and configuration as the macrointercalant chains. Unfortunately, preparation of such organoclays is complex and expensive.[14]

It is pertinent to describe briefly elements of the PP-based PNC technology. The principal method used in the industrial and academic laboratories is based on the use of reactive compatibilizers. In 1997, Usuki et al.[15] prepared PP-based PNC using a standard organoclay (MMT intercalated with quaternary ammonium ion) melt compounded with PP and maleated PP (PP-MA). The latter polymers have been known in the plastics industry as coupling or compatibilizing agents for polymer blends (e.g., PP/PA), polymer composites (e.g., PP with glass fiber), manufacture of high-quality "plastic wood", etc.

Owing to the wide variety of commercially available PP-MA grades (molecular weight, polydispersity, number of maleic anhydride groups per chain, contamination by coreactants, homopolymerized MAH, etc.), its selection for PNC compatibilization is far from simple. The main concern is the balance between the degree of maleation and molecular weight. High molecular weight of PP-MA required for efficient compatibilization means a low degree of maleation. As the degree of maleation increases, bonding to the clay surface improves, but the compatibilizer miscibility with PP decreases! The polar MAH groups have a tendency to cluster into micelles dispersed in a hydrocarbon matrix; thus, the concentration and process variables must be selected to ascertain grafting to the clay surface while minimizing micellization.

For example, Kato et al.[16] reported that PP-MA with acid value $A\# = 52$ worked quite well, but that with $A\# = 7$ mg KOH/g not at all. In another publication[17] it was shown that PP-MA with acid value $A\# = 52$ phase separated from PP, but the one with $A\# = 26$ mg KOH/g did not. Hasegawa et al.[18] well dispersed MMT (interlayer spacing: $d_{001} = 6.3$ nm) by first melt compounding organoclay with PP-MA ($A\# = 52$ mg of KOH/g) at a ratio $\Xi = 1{:}3$ and then diluting the master batch with PP to clay content of ca. 5.0 wt %. The performance deteriorated if during the first step lower ratio, $\Xi < 1{:}3$, was used. The authors stressed the two critical conditions for clay dispersion: (1) strong interaction of PP-MA with the organoclay and (2) miscibility of the PP-MA macromolecular chains with the matrix PP. More recently, full exfoliation was reported for PNC's containing organoclay dispersed in a variety of PP-MA matrixes.[19] Owing to the absence of PP, the problems associated with miscibility were absent.

In the above-summarized series of publications the principal organoclay was MMT intercalated with octadecylammonium ion (MMT-C18), and melt compounding was carried out at 200 °C. The use of primary ammonium ion may be important as the three hydrogens of RNH_3^+ cation may react with the maleic anhydride group. Furthermore, the selected low compounding temperature may also be important, as the thermal degradation of organoclays is a major problem at temperatures exceeding ca. 180 °C.[20−27] Clay is also known for its catalytic activity;[28] thus, the exposed surface of clay platelet may accelerate the thermal degradation of the matrix polymer.[29] It is noteworthy that the mechanism of reaction between organoclay and PP-MA remains unknown. Several possible chemical reactions are possible, viz. with ammonium cation, or clay −OH groups (covalent or hydrogen bonding). If the latter reaction is the dominant one, than reaction with the −OH groups on or near the platelet edge may be responsible for a partial blocking the interlamellar gallery space, thus slowing down the clay dispersion.

An alternative series of PP-based PNC has been formulated using clays intercalated with quaternary ammonium ion—either commercial or homemade, purified by extraction or not.[30−36] The common observation for these intercalated systems is that the interlayer spacing rarely exceeds $d_{001} = 3.6$ nm. The problem may be associated with inadequate reaction between the MAH groups of the compatibilizer and the −OH groups of the clay, the thermal degradation of organoclay that inhibits diffusion of the compatibilizer to clay galleries, or clay concentration in the noncrystalline regions of the nanocomposites. However, considering the cost and commercial availability of variety of quaternary ammonium organoclays, the effort to solve these problems continues.

These aspects have been considered in preparing the PNC systems for the current investigations. The work described in this publication attempts to examine (1) applicability of the HCP model to PP-based PNC, (2) correlation between the free volume function h and clay interlayer spacing, viz. $d_{001} = f(\Delta h)$, and (3) applicability of the developed *PVT* data evaluation for systems containing matrix, MMT, intercalant, and compatibilizer. A more general aim of this work has been to demonstrate the usefulness of *PVT* measurements for understanding the interactions and structures present within the molten PNC.

II. Experimental Section

The polymeric components of the studied PNC are listed in Table 1. The organoclay was MMT intercalated with 0.78 mmol/g of dimethyl dihydrogenated tallow ammonium chloride (Cloisite 15A from Southern Clay Products, Gonzales, TX; $d_{001} = 2.96$ nm; abbreviated as C15). One PNC specimen was prepared by melt compounding 3 wt % Cloisite 6A (similar to C15 as it also contains dimethyl dihydrogenated tallow ammonium ions, but in larger amount—0.86 mmol/g; n.b., C6A is no longer available) with PP.

The neat polymer and its PNC were compounded in a corotating Leistritz twin-screw extruder (TSE), $D = 34$ mm, $L/D = 40$, at 100 or 200 rpm, with the high-shear screw

Table 2. Composition and Properties of PP-Based PNC Samples

no.	code[a]	V_0(RT)[b] (mL/g)	C15 (wt %)	MMT[d] (wt %)	M_s (g/mol)	P^* (bar)	10^4V^* (mL/g)	T^* (K)	r^2	σ
Z	PPz	1.1148	0	0	40.8	6043 ± 79	11827 ± 24	10535 ± 56	0.999 997	0.002 04
0	PPo	1.1107	0	0	50.5	4973 ± 113	11932 ± 42	10804 ± 117	0.999 998	0.001 71
1	PP	1.1424	0	0	43.1	5727 ± 68	11728 ± 22	10449 ± 57	0.999 998	0.001 65
2	PP-2	1.1030	2	1.1	48.4	5169 ± 103	11874 ± 37	10712 ± 98	0.999 998	0.001 92
3	PP-3	1.1038	3[c]	1.76	46.7	5457 ± 55	11712 ± 18	10775 ± 49	0.999 998	0.001 84
4	PP-2-E43	1.1005	2	1.13	49.4	5230 ± 117	12060 ± 42	11251 ± 120	0.999 996	0.002 50
5	PP-2−315	1.0980	2	1.17	51.9	4923 ± 99	11971 ± 37	10970 ± 101	0.999 996	0.002 48
6	PP-2-GMA	1.1042	2	1.23	47.8	5247 ± 95	11993 ± 34	10848 ± 90	0.999 997	0.002 26
7	PP-4	1.1018	4	2.42	50.7	5028 ± 93	11857 ± 34	10917 ± 92	0.999 997	0.002 27
8	PP-E43	1.0921	0	0	49.2	5111 ± 95	11926 ± 34	10820 ± 91	0.999 997	0.002 35
9	PP-4-E43	1.0900	4	2.19	43.4	5826 ± 117	11662 ± 37	10647 ± 96	0.999 996	0.002 58
10	PP-4−315	1.0906	4	2.12	48.5	5266 ± 93	11931 ± 33	10993 ± 91	0.999 996	0.002 55
11	PP-4-GMA	1.0894	4	2.15	49.4	5203 ± 96	11807 ± 34	10952 ± 94	0.999 997	0.002 27

[a] In the column: PPz indicates PP homopolymer (ProFax 6523 from Hercules)[38] and PPo is virgin resin, while extruded as PP. PP-2, PP-3, and PP-4 are binary PNC systems. For other samples the code, PP-*X*-comp, indicates PNC containing $X = 2$ or 4 wt % of C15 and 2*X* of compatibilizer: E43, 315, or GMA (see Table 1). [b] V_0 is the specific volume under ambient conditions ($T = 22-25$ °C). [c] The sample no. 3 contains 3 wt % of C6. [d] The MMT column lists the inorganic content (accuracy ±2%) after pyrolysis in air at temperatures up to 700 °C; the samples were heated at a rate of 20 °C/min to 700 °C and keep at it for 100 min. M_s is the molecular weight per statistical segment (see eq 1). Columns 5−8 list the *PVT* characteristic parameters and the last two columns the correlation coefficient squared (r^2) and the standard deviation (σ) of the *PVT* data fit to S−S eos.

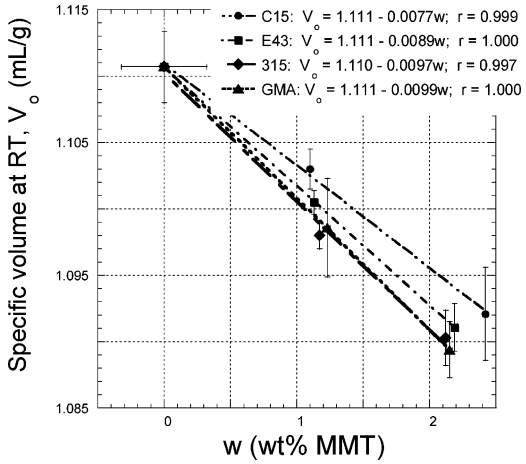

Figure 1. Specific volume under ambient conditions vs inorganic clay (MMT) content for the four systems of Table 2.

configuration at $T = 180-200$ °C. Prior to testing, the samples were dried under vacuum at 90 °C for at least 48 h. The organoclay was fed from a side feeder. The compositions of the PNC samples are listed in Table 2.

The *PVT* behavior was measured in a Gnomix apparatus (Gnomix Inc., Boulder, CO), within the range of temperatures, $T = 300-590$ K, and pressures, $P = 0.1-190$ MPa. The molten state was observed within at temperatures from about 450 to 530 K. Since the instrument measures only the incremental specific volume changes, ΔV, as a function of P and T, first the absolute value of V (with accuracy $\geq \pm 0.001$ mL/g) under ambient conditions was measured in a glovebox, under positive pressure of dry N_2. As shown in Figure 1, the ambient specific volume decreases linearly with inorganic content. The slopes, $dV_0/dw = \sum V_{0i}w_i$, are related to the weight-average specific volume of the organic components—the lowest slope is for the binary PNC containing only PP and C15, and the higher were obtained for systems with styrene-containing compatibilizers having higher density than PP.

To ascertain reliability of data, for each sample at least two "isothermal" runs were carried out—the tests were repeated if the difference of ΔV between two consecutive runs was greater than ±0.0002 mL/g. In consequence, some of the samples were measured up to six times. During the "isothermal" runs the temperature is set and $V = V(P)$ is measured, then T increases to the next level (usually 10 °C higher), and the process is repeated. Thus, the specimen is exposed to the highest temperature only at the end of the test.

III. Theory

The Simha−Somcynsky lattice−hole theory models an amorphous, condensed system as a mixture of sites occupied by chain segments (or small molecules) and empty sites—a measure of disorder. The configurational entropy of mixing is expressed in the manner of Huggins and Flory. The intersegmental interactions are described by a 6−12 potential with a maximum attraction energy, ϵ^*, and repulsion volume, v^*. The Lennard-Jones−Devonshire (L−J) cell potential is approximated by a square well. Following the original proposal by Prigogine and colleagues, a number 3*c* of external, volume-dependent degrees of freedom is assigned to each solvent molecule or polymeric s-mer.

The variables of state, and all derived quantities, such as the *PVT* surface (eos), or the cohesive energy density (CED), are scaled, and a theorem of corresponding states for large *s* results. For the macromolecular species: $3c/s \Rightarrow 1$ is usually assumed. The three characteristic scaling parameters of pressure, temperature, and volume are expressed respectively as

$$\left.\begin{aligned} P^* &= zq\epsilon^*/(sv^*) \\ T^* &= zq\epsilon^*/(Rc) \\ V^* &= v^*/M_s \end{aligned}\right\} (P^*V^*/T^*)M_s = Rc/s \Rightarrow R/3 \quad (1)$$

with M_s the molar segmental mass, $zq = s(z-2)+2$ the number of interchain contacts in a lattice of coordination number $z = 12$, and R the gas constant. In this manner a scaled configurational free energy in reduced variables (indicated by tilde) is derived:

$$\tilde{F} \equiv F/F^* = \tilde{F}[\tilde{V},\tilde{T},h(\tilde{V},\tilde{T})] \quad (2)$$

At thermodynamic equilibrium the vacancy (hole) fraction $h = h(\tilde{V}, \tilde{T})$—a measure of free volume—is obtained by minimization of $\tilde{F}$:

$$(\partial\tilde{F}/\partial h)_{\tilde{V},\tilde{T}} = 0 \quad (3a)$$

Equations 2 and 3a determine the configurational

thermodynamic properties of the system. In particular, they define the reduced equation of state, eos, using the customary definition

$$\tilde{P} = -(\partial \tilde{F}/\partial \tilde{V})_{\tilde{T}} \quad (4a)$$

Thus, the S−S eos is expressed by the coupled eqs 3a and 4a, written in explicit form as

$$3c[(\eta - {}^1/_3)/(1-\eta) - yQ^2(3.033Q^2 - 2.409)/6\tilde{T}] + (1-s) - s\ln[(1-y)/y] = 0 \quad (3)$$

$$\tilde{P}\tilde{V}/\tilde{T} = (1-\eta)^{-1} + 2yQ^2(1.011Q^2 - 1.2045)/\tilde{T} \quad (4)$$

with the occupied site fraction $y = 1 - h$, $Q = 1/(y\tilde{V})$, $\eta = 2^{-1/6}yQ^{1/3}$. Finally, with the assumption $3c/s \rightarrow 1$ for polymeric melts, the equivalent segmental molar mass, M_s (defined by eq 1), may be calculated once the numerical values of the scaling parameters have been extracted from experiment. Thus, eqs 3 and 4 not only describe the *PVT* surface, but associated to it the free volume function: $h = h(\tilde{V}, \tilde{T})$. Polynomial approximations of their solutions are available.[6]

The single-component theory has been extended to multicomponent mixtures. Under random mixing conditions, eqs 3 and 4 were shown to be valid, provided that the interaction parameters ϵ^* and v^* in eq 1 are replaced by compositional averages, $\langle\epsilon^*\rangle$ and $\langle v^*\rangle$. For two components these depend on the binary "11", "12", and "22" interaction parameters as

$$\langle\epsilon^*\rangle/\langle v^*\rangle^p = X_1{}^2\epsilon^*_{11}\, v^{*p}_{11} + 2X_1X_2\epsilon^*_{12}\, v^{*p}_{12} + X_2{}^2\epsilon^*_{22}\, v^{*p}_{22}; \quad p = 2,4 \quad (5)$$

where the site fractions, X_1 and $X_2 = 1 - X_1$, are defined in terms of the mole fractions x_i:

$$X_1 = zq_1x_1/(zq_1x_1 + zq_2x_2) \quad (6)$$

The two exponents in eq 5, $p = 2$, 4, reflect the L−J "6−12" pair potential. Thus, to fully describe the *PVT* dependence of two-component systems, six binary interaction parameters are required. Since these are interrelated by the two relations in eq 5, one needs at least four additional sets of information. These may be generated by experiment (e.g., *PVT* data at different concentrations) and/or by additional assumptions consistent with the lattice−hole model.

The optimum value of the reducing parameters (P^*, T^*, and V^*) is determined by simultaneously fitting the experimental *PVT* surface in the molten state to eqs 3 and 4. In this work, the commercial software (Scientist from MicroMath) was used to optimize the fit. The program uses the nonlinear least-squares algorithm to compute the reducing parameters by minimization of the differences between experimental data and the theory. A rapid convergence is obtained using a two-step approach: (1) An initial fitting to the polynomial expression $\tilde{V} = \tilde{V}(\tilde{P}, \tilde{T})$ provides the initial values of P^*, T^*, and V^* parameters for the subsequent iterations. (2) Fitting the data to the coupled eqs 3 and 4. Usually 20−40 iterations were required for convergence with consecutive errors of $\Sigma\tilde{V} = 10^{-7}$. The fitting provides numerical values of the hole fraction, $h = h(\tilde{P},\tilde{T})$, as well as the parameters P^*, T^*, and V^*, from which the bulk average interaction parameters may be calculated using the definitions in eq 1.

IV. Model of Molten PNC

To calculate the binary interaction parameters ϵ^*_{ij}; v^*_{ij} ($i, j = 1, 2$) from their averages, $\langle\epsilon^*\rangle$ and $\langle v^*\rangle$, the HCP model[2] was adopted. As stated in the Introduction, the model assumes a reduction of molecular mobility near a crystalline surface. This type of "solidification" was predicted by molecular dynamics and experimentally measured.[7−9,39,40] The reported extent of solidification from solution or from melt has been remarkably similar. Furthermore, the model was quite successful for interpretation of not only the *PVT* behavior[2] but also the strongly nonlinear viscoelastic flows.[41] Accordingly, the limiting distances from the clay platelet of the solidified organic phase, $z_0 = 6$ nm, and that of the variable matrix properties $z_\infty = 100$ nm are adopted.

Calculations of the six binary interaction parameters from the two dependencies of eq 5 require additional information—experimental data and/or justifiable assumptions. The four PNC series were prepared with at least three organoclay concentrations: 0, 2, and 4 wt %; thus, for ideal systems the single valued interaction parameters may be computed. However, there is a need to estimate the always-present error. Furthermore, the HCP model assumes that the matrix properties vary with the average distance from clay surface, $6 \le z \le 100$ nm. In short, additional assumptions are needed.

The cross-interaction parameters, ϵ^*_{12} and v^*_{12}, may be approximated by the geometric (Berthelot's rule) and algebraic averages, respectively:

$$\epsilon^*_{12} = \sqrt{\epsilon^*_{11}\,\epsilon^*_{22}} \quad \text{and} \quad \epsilon^*_{11} = [v^{*1/3}_{11} + v^{*1/3}_{22}]^3/8 \quad (7)$$

Thus, knowing ϵ^*_{11}; v^*_{11} and ϵ^*_{22}; v^*_{22} the mixed parameters (ϵ^*_{12}; v^*_{12}) can be calculated. In the following part the index 22 refers to the clay platelets enrobed by solidified polymer.

The *PVT* measurements of neat PP provide ϵ^*_{11} and v^*_{11} of the matrix far away from the clay surface, i.e., at a distance: $z > z_\infty = 100$ nm. From a geometrical argument (assuming exfoliation) this may be expected in diluted PNC systems containing $w \le 1.2$ wt % of clay or $w \le 2.1$ wt % of C15. Thus, the assumption of a solidified layer on the surface of MMT platelet embedded in a polymeric matrix still requires a functional description of the property changes within the distance from z_0 to z_∞. Arbitrarily, the following exponential function was adopted:

$$y(z) = \frac{y_0 y_\infty}{y_0 - (y_0 - y_\infty)\exp\{n[(z - z_0)/(z - z_\infty)]\}}; \quad z_0 \le z < z_\infty \quad (8)$$

In eq 8, y_0 represents the matrix interaction parameters, $\epsilon^*_{11}(z)$ or $v^*_{11}(z)$, at the solidified polymer layer (at $z_0 = 6$ nm). For large values of z (approaching the upper limit of eq 8: $z_\infty = 100$ nm), the exponential term becomes negligible compared to y_0 and y approaches a constant value of y_∞, characteristic of the neat matrix. Thus, at the lower limit: $y(z) = y_0$ becomes $\epsilon^*_{11}(z) = \epsilon^*_{22}$, and $v^*_{11}(z) = v^*_{22}$, while for the upper, the characteristic values of the matrix are obtained: $\epsilon^*_{11}(z) = \epsilon^*_{11}$ and $v^*_{11}(z) = v^*_{11}$. Figure 2 illustrates the dependence for a

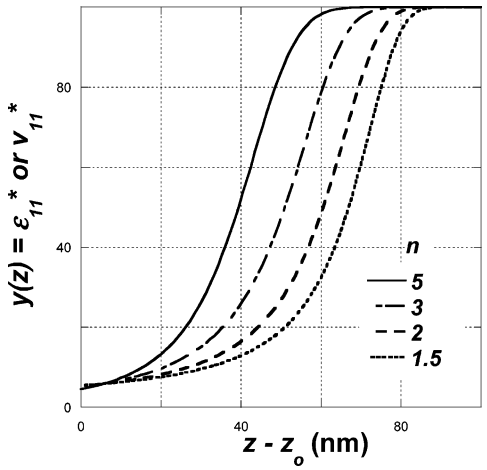

Figure 2. Variation of the matrix interaction parameters, ϵ^*_{11} or v^*_{11}, as a function of distance z from the MMT surface (see eq 8).

series of n values, within the arbitrarily chosen abscissa limits: $6 \le y(z) < 100$. The magnitude of n affects the predicted rate of change in the z-direction of the interaction parameters, $\epsilon^*_{11}(z)$ and $v^*_{11}(z)$, but not the limiting values. For the further computations the value $n = 2$ was selected.

The z-dependent $\epsilon^*_{11}(z)$ and $v^*_{11}(z)$ parameters are computed for one-half of the average distance between clay platelets, which depends on concentration. To calculate its magnitude, it was assumed that the clay platelets are randomly placed in the matrix, and the average thickness of the organic layer can be calculated from the geometry:

$$\langle z \rangle = (d^{C15}_{001}\rho_{C15}/\rho_{matrix})(1/m_2 - 1) \qquad (9)$$

where d^{C15}_{001} is the interlayer spacing in C15, ρ_{C15} and ρ_{matrix} are densities of C15 and the matrix, respectively, and m_2 is the weight fraction of clay. A computer program compares this average value with the boundary conditions of eq 8 and for the values $6 \le \langle z \rangle/2 < 100$ equates $\langle z \rangle/2$ with z in eq 8; for $\langle z \rangle/2 > 100$ the values of the matrix are taken. The program optimizes the fit of the "experimental" (i.e., extracted from P^*, V^*, T^*) bulk average parameters, $\langle \epsilon^* \rangle$ and $\langle v^* \rangle$, to eqs 5−9, yielding the interaction parameters, ϵ^*_{22} and v^*_{22}, as well as the concentration-dependent interaction parameters of the matrix, $\epsilon^*_{11} = \epsilon^*_{11}(X_1)$ and $v^*_{11} = v^*_{11}(X_1)$.

Evidently, the magnitude of the computed parameters depends on the assumptions, viz. validity of eq 7, the matrix interactions profile, eq 8, and the values of its parameters, n, z_0, and z_∞. Changing these will change the numerical values, but neither the relative magnitude of computed parameters nor the validity of the adopted HCP model. The model provides a common basis for the interpretation of PNC thermodynamic and rheological behavior.

V. Calculations

The characteristic reducing parameters (P^*, T^*, and V^*) for the PP-based PNC were computed from the multiple tests of each composition fitted to the coupled eqs 3 and 4. Their values, along with the statistical fit data, are listed in Table 2. As is evident from the last two columns, in all cases a good fit of data to the S−S eos was obtained. An example illustrating the reproducibility of measurements, and goodness of fit to eos is shown in Figure 3.

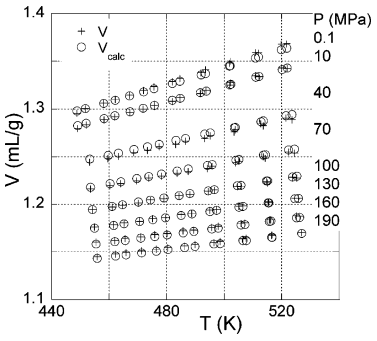

Figure 3. Example of eqs 3 and 4 fit to two sets of PVT measurements for PP-4-GMA. Crosses and circles are experimental and computed from S−S eos, respectively.

To calculate the binary interaction parameters, ϵ^*_{ij}; v^*_{ij} ($i, j = 1, 2$) of eq 5 from their averages, $\langle \epsilon^* \rangle$ and $\langle v^* \rangle$, the molar and site fractions (x_i, and X_i, respectively) must be known. The molar fraction of the polymeric matrix, x_1, is reduced by solidification on the clay platelet:

$$x_1 = \frac{(m_1/M_{s1}) - (m_{1,solid}/M_{s1})}{(m_1/M_{s1}) + (m_2/M_{s2})} \qquad (10)$$

where m_1 is the weight fraction of the polymers, $m_{1,solid}$ is the weight fraction of solidified matrix, m_2 is the weight fraction of clay, and $M_{si} = M_i/s_i$ is the molecular weight of statistical segment of component "i" (M_i and s_i are molecular weight and number of statistical segments, respectively). Fitting *PVT* data to eos gives $M_{s1} = 43.115$ for the PP used in this work (see no. 1 in Table 2), whereas the molecular weight of PP-mer is $M_0 = 42.081$ g/mol. Thus, one lattice cell accommodates about one hard-core statistical segment of PP with the molecular volume of $v^*_{hard} = 43.115/2^{1/2} = 30.49$ mL/mol and one hard-core statistical segment of clay of a similar volume. The latter rule provides the means for computing the molecular weight of the clay statistical segment, M_{s2}.

The "molecular mass" of clay platelet having diameter $d = 100$ nm, thickness $h = 0.96$ nm, and density $\rho = 2.3$ g/mL is $M_2 = N_A\rho\pi d^2 h/4 = 10\,443$ (kg/mol), and its "molecular volume" is $V_{plat} = M/\rho = 4.54 \times 10^6$ mL/mol. In consequence, the number of segments for PP (s_1) and clay (s_2) are respectively $s_1 = 4871$ and $s_2 = V_{plat}/v^*_{hard} = 1.489 \times 10^5$. Finally, the mass of solidified polymer can be calculated from the mass of clay and relative volume of clay to solidified polymer: $m_{1,solid} = m_2(12A\rho_1)/(0.96A\rho_2) = 4.892m_2$. Computations for the two-component system (PP + C15) resulted in the dependencies shown in Figures 4 and 5. The error of measurements for ϵ^*_{22} and v^*_{22} is respectively ±4.0 and ±2.0%.

It can be seen in Figure 4 that the bulk-averaged interaction parameter for the PNC system with 3 wt % C6 (clay content 1.76 wt %) does not follow the dependence observed for PNC with C15. The deviation may be caused by difference in organoclay composition (C15A and C6A contain 1.25 and 1.40 dimethyl dihydrogenated tallow ammonium ion, respectively), the thermal degradation, and/or phase separation of intercalant. For these reasons, the composition containing C6 organoclay will be excluded from further considerations.

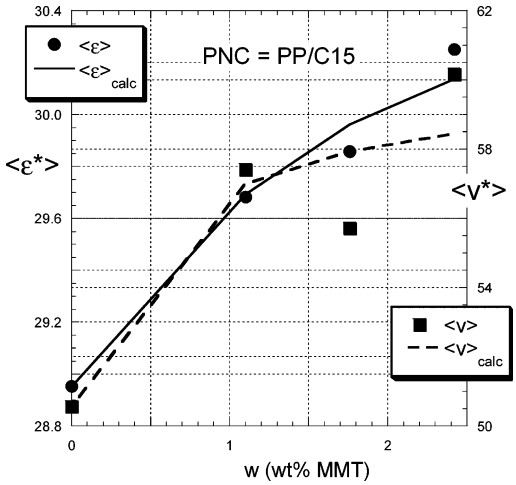

Figure 4. Bulk-average interaction parameters as functions of clay content for the binary system of PP with Cloisite 15A. The values extracted from the *PVT* data are shown as points, with the calculations as lines.

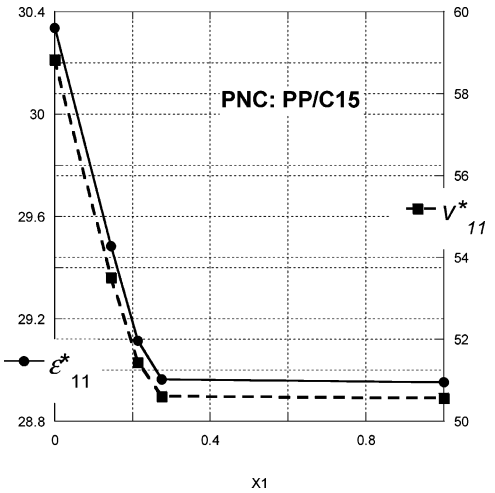

Figure 5. Changes of the matrix (PP) interaction parameters (away from the solidified layer) as functions of the PP site fraction, X_1. The dependencies were computed from the raw data in Figure 4.

Similar computations were carried out for the PNC with compatibilizer. Here the basic assumption is that the compatibilizer is miscible with the matrix and intercalant; thus, the three organic substances (intercalant, PP, and compatibilizer) form a matrix. The bulk-average values of the interaction parameters, $\langle\epsilon^*\rangle$ and $\langle v^*\rangle$ (calculated from the characteristic reducing parameters: P^*, T^*, V^*), and the values computed from the HCP model are listed in Table 3 and shown in Figures 6 and 7, respectively. In Table 3, the concentration-dependent binary interaction parameters for the average matrix, $\epsilon^*_{11} = \epsilon^*_{11}(X_1)$ and $v^*_{11} = v^*_{11}(X_1)$, are also presented. The model well describes the behavior in the two-component system (PP + C15) and a three-component system containing GMA but shows deviations for the remaining two PNC's, compatibilized with either E43 or 315.

Interactions within PNC. The statistics of the data fit to the HCP model for the four PNC systems (standard deviation, σ, the correlation coefficient squared, r^2, and correlation of determination, *CD*) is presented in Table 4 along with the binary interaction parameters for the clay platelets enrobed with solidified organic phase, ϵ^*_{22} and v^*_{22}, as well as for the matrix at $z > 100$ nm, ϵ^*_{11} and v^*_{11}. The heterogeneous interaction parameters, ϵ^*_{12} and v^*_{12}, were calculated from eq 7. The model well describes interactions in the PP + C15 and PP + C15 + GMA systems, but as expected, poorly in systems compatibilized with E43 and 315 (see also Figures 6 and 7).

The Hole Fraction. The hole fraction, h, is an integral part of the S−S eos. Thus, fitting the *PVT* data to the coupled eqs 3 and 4 provides the h values corresponding to any pair of independent variables. Alternatively, knowing the characteristic reducing parameters, P^*, T^*, V^*, one may compute V and h at any P and T. Results of such computations for the four series of PP-based PNC are displayed in Figure 8. Within the full temperature range the dependencies are parallel to each other. At any temperature PP has the highest hole fraction—all the PNC compositions show lower levels of h.

An alternative method of analyzing the effects of adding organoclay to a polymer is to plot the relative values of specific volume and hole fraction:

$$V_r = V(\text{PNC})/V(\text{PP})|_{P,T=\text{const}}; \quad h_r = h(\text{PNC})/h(\text{PP})|_{P,T=\text{const}} \quad (11)$$

Figure 9 shows these functions for the PP/C15 system, with organoclay loading of 2 and 4 wt % at constant pressure of $P = 10$ MPa and at temperatures ranging from 450 to 550 K. While V_r changed little (≤1%), incorporation of 1.1 and 2.42 wt % of MMT reduced h_r at $T = 500$ K to 0.953 and 0.920, respectively.

The concentration dependence of the hole fraction at $P = 10$ MPa and $T = 500$ K for the four PNC systems is displayed in Figure 10. Here the Δh decrement is defined as

$$\Delta h \equiv 100[h(\text{PP}) - h(\text{PNC})]/h(\text{PP})|_{P,T=\text{const}} = 100(1 - h_r) \quad (12)$$

Similarly as for the bulk-averaged interactions in Figures 6 and 7, here also a regular increase of Δh is observed for the binary PP + C15 system and for PP + C15/+GMA. Strong nonmonotonic variations are observed for the system compatibilized with Epolene-43 and with Polybond-3150.

VI. Discussion

The *PVT* experimental data for PP and four PP-based PNC systems were fitted to the Simha−Somcynsky eos. For all specimens the theory described well the experimental data, with the correlation coefficient squared, $r^2 \geq 0.999\,996$, and the standard deviation, $\sigma \leq 0.002$. The fitting provided two types of information: (1) the characteristic, reducing parameters (P^*, T^*, V^*) dependent on the bulk-average interaction parameters, $\langle\epsilon^*\rangle$ and $\langle v^*\rangle$, and (2) the free volume function, $h = h(P,T)$.

Interactions. To extract the binary interaction parameters from the bulk quantities, $\langle\epsilon^*\rangle$ and $\langle v^*\rangle$, the HCP model was used. The model assumes the presence of a 6 nm thick layer of "solidified" organic phase on the surface of the clay platelet and of a matrix with chain mobility increasing with distance from the clay surface, $z = 6-100$ nm. Only above the upper limit may the properties of neat matrix be recovered. It is note-

Table 3. Experimental and Computed Average Interaction Parameters for the Four PP-Based PNC Systems[a]

system	% MMT	$\langle\epsilon^*\rangle$	$\langle v^*\rangle$	$\langle\epsilon^*\rangle_{calc}$	$\langle v^*\rangle_{calc}$	$\epsilon^*_{11}(z)$	$v^*_{11}(z)$	X_1
C15	0	28.954	50.565	28.954	50.565	28.954	50.565	1
	1.1	29.683	57.427	29.693	56.998	28.964	50.615	0.2747
	2.42	30.251	60.172	30.138	58.452	29.484	53.522	0.1444
						30.337	58.840	0.0
E43	0	28.958	50.565	28.954	50.565	28.954	50.565	1
	1.13	31.179	59.615	30.355	55.761	28.954	50.565	0.3548
	2.19	30.097	53.506	30.816	56.769	29.278	51.419	0.2094
						31.54	58.12	0.0
315	0	28.958	50.565	28.954	50.565	28.954	50.565	1
	1.17	30.401	61.752	30.178	58.955	28.954	50.565	0.3463
	2.12	30.465	57.853	30.702	60.310	29.211	51.691	0.2156
						31.68	62.35	0.0
GMA	0	28.958	50.565	28.954	50.565	28.954	50.565	1
	1.23	30.063	57.295	30.020	57.307	28.954	50.565	0.3343
	2.15	30.353	58.341	30.389	58.335	29.205	51.570	0.2129
						31.11	60.02	0.0

[a] The values $\langle\epsilon^*\rangle$ and $\langle v^*\rangle$ are extracted from fitting S−S eos to the experimental *PVT* data, while their analogues in angular brackets are calculated from the HCP model. The latter calculations also yield the concentration-dependent values of the matrix interaction parameters, $\epsilon^*_{11}(z)$ and $v^*_{11}(z)$.

Table 4. Statistics of Data Fit to the Bulk-Average Interaction Parameters for the Four PP-Based PNC Systems

parameter	PP + C15	PP + C15 + E43	PP + C15 + 315	PP + C15 + GMA
σ	0.391	2.584	1.868	0.028
r^2	0.999950	0.997716	0.998875	0.9999997
CD	0.999722	0.985810	0.993876	0.999998
ϵ^*_{22}	30.88 ± 0.38	31.54 ± 2.57	31.68 ± 1.87	31.11 ± 0.03
v^*_{22}	61.35 ± 0.34	58.12 ± 2.32	62.35 ± 1.63	60.02 ± 0.02
ϵ^*_{11}(PP)	28.95 ± 0.16	28.95 ± 0.16	28.95 ± 0.16	28.95 ± 0.16
v^*_{11}(PP)	50.57 ± 0.09	50.57 ± 0.09	50.57 ± 0.09	50.57 ± 0.09
ϵ^*_{12}	29.90 ± 0.54	30.22 ± 2.66	30.28 ± 2.03	30.01 ± 0.12
v^*_{12}	55.79 ± 0.43	54.26 ± 2.41	56.25 ± 1.72	55.16 ± 0.11

worthy that in 1 g of PNC containing 2 wt % of C15 there are about 8 million platelets with the total surface area of ca. 13 m^2, capable to "solidify" 9% of matrix and significantly reducing mobility (hence the free volume) of the rest. A computer program fitted eqs 5−8 to the full sets of data (three concentrations for each PNC system) by the nonlinear least-squares method. Figures 4−7 and Tables 3 and 4 summarize the results.

The HCP model well describes the binary system (PP + C15) and the one compatibilized with GMA-grafted PP, but deviations are noted for PNC compatibilized with Epolene-43 and (to a lesser degree) for the one with Polybond-3150. Comparing Figure 6 with Figure 7 indicates that even stronger variations from the expected behavior are observed for $\langle v^*\rangle$.

It has been noted[42] that for a series of polymers belonging to the same family, e.g., PS with different molecular weights, a variety of polydispersity or commercial additives, the interaction parameters v^* and ϵ^* are linearly related to each other. The correlation is not universal, as different polymers follow different linear dependencies. Figure 11 displays this correlation for the four PP-based PNC. Large scattering is observed for the PNC containing Epolene-43 and a smaller for the one compatibilized with Polybond-3150. Good linearity is noted for the binary system (PP + C15) and for the one compatibilized with GMA-grafted PP.

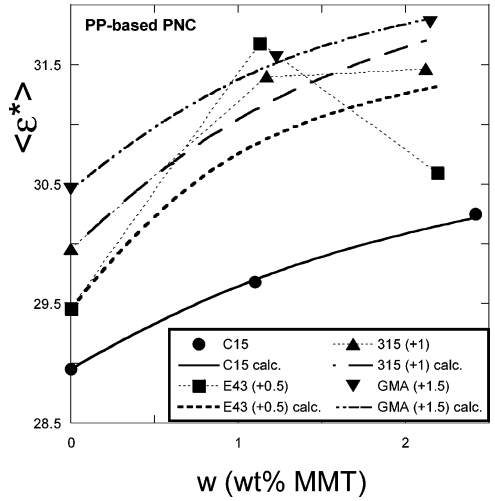

Figure 6. Energetic, bulk-average interaction parameters and their computed values for four systems (from the bottom): PP + C15; PP + C15+E43; PP + C15+315; and PP + C15 + GMA. For clarity, each set was shifted up by 0.5 unit.

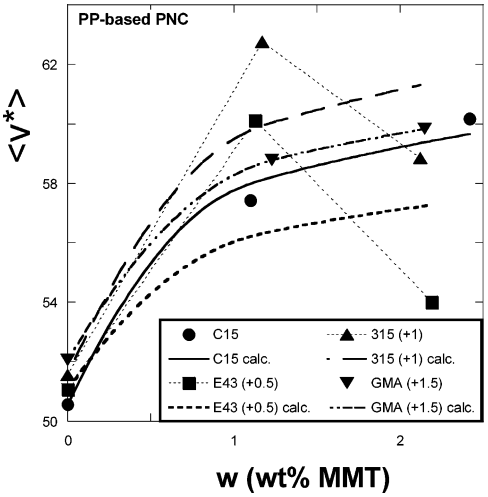

Figure 7. Volumetric, bulk-average interaction parameters and their computed values for four systems (from the bottom): PP + C15; PP + C15 + E43; PP + C15 + 315; and PP + C15 + GMA. For clarity, each set was shifted up by 0.5 unit.

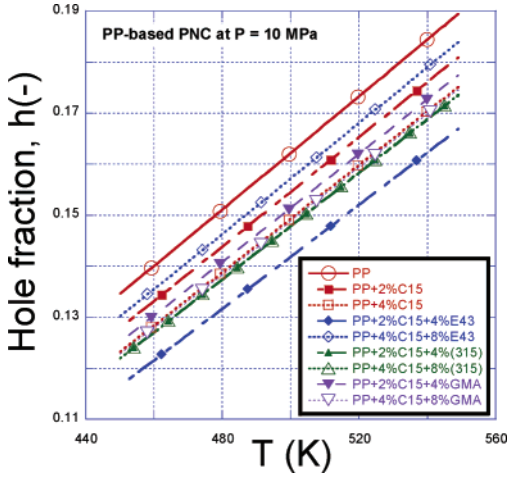

Figure 8. Hole fraction h vs T at $P = 10$ MPa vs temperature for the four series of PP-based PNC. Full and empty symbols are for 2 and 4 wt % organoclay, respectively.

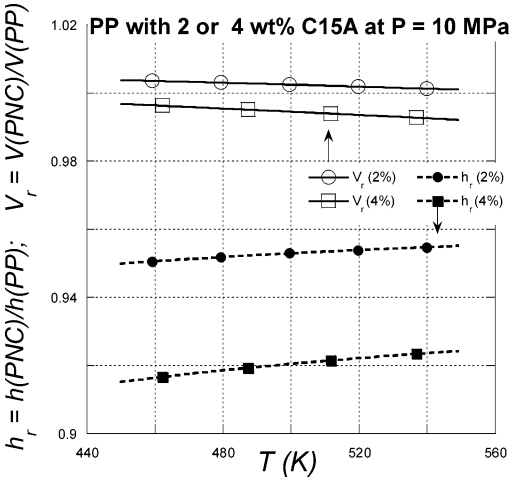

Figure 9. Relative specific volume and hole fraction for PP-based PNC containing 2 and 4 wt % of C15.

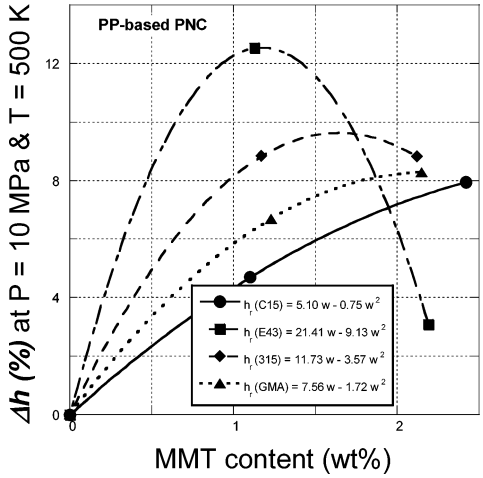

Figure 10. Reduction of the hole fraction (at $P = 40$ MPa and $T = 500$ K) as a function of clay content for the four PP-based PNC.

Free Volume. The differences in behavior of the interaction parameters are also apparent in the hole fraction dependencies shown in Figures 8−10. The latter figure displays the magnitude of the hole fraction decrease, Δh, caused by addition of organoclay. Qualitatively, the data in Figure 10 are in agreement with

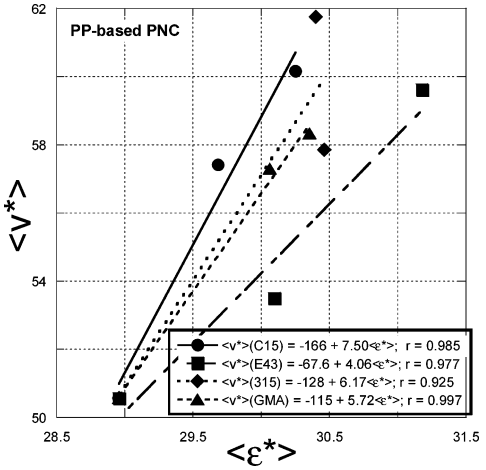

Figure 11. "Experimental" bulk-average interaction parameters $\langle v^* \rangle$ vs $\langle \epsilon^* \rangle$ for the four PP-based PNC.

the behavior of the bulk-average interaction parameters shown in Figures 6 and 7, as discussed in the preceding part.

The adopted HCP model predicts that solidification on the clay platelets results in reduced free volume. Furthermore, since in exfoliated (i.e., diluted PNC) the accessible clay surface area is proportional to organoclay loading, the reduction of the matrix h-fraction caused by addition of 4 wt % of C15 is expected to be twice as large as that observed for PNC with 2 wt % C15 (for intercalated PNC smaller changes in Δh are expected). The data for PP + C15 system almost fulfill the former expectation. Incorporating 1.1 and 2.42 wt % of MMT reduced the matrix free volume (at $P = 10$ MPa and $T = 500$ K) by $\Delta h = 4.7$ and 8.0%, respectively. The small deviation from linearity (see Figure 10) may be due to reduction of the degree of clay dispersion caused by crowding.

Figure 10 shows that the linear relation between Δh and clay loading is not universal. Initially, addition to PP of 2 wt % C15 + 4 wt % compatibilizer reduces the free volume, Δh, in a sequence: Δh(none) = 4.70, Δh(GMA) = 6.69, Δh(315) = 8.84, and Δh(E43) = 12.5%. However, doubling the amount of these additives produces a dramatic decrease of Δh for E43, no change for 315, a small increase for GMA, and (as discussed above) nearly the expected doubling of the Δh value for PP + C15.

For a single-component system one may expect a correlation between the Lennard-Jones interaction parameters and the hole fraction, h. As shown in Figure 12, such a correlation has been also found for the PP-based PNC's containing either 2 or 4 wt % C15. Here, the values of h computed from the eos (at $P = 10$ MPa and $T = 500$ K) are plotted vs the bulk-average energetic interaction parameter $\langle \epsilon^* \rangle$, giving a high correlation coefficient, $r = 0.997$. Evidently, similar correlations are expected using h at other P and T pairs within the molten matrix region. Despite the structure and interaction differences within the specimens, the theory is self-consistent. Hence, either the interaction parameters or the hole fraction may be used for correlating the *PVT* behavior with other physical characteristics of the systems, viz. the interlayer spicing, d_{001}, mechanical performance, permeability, etc.

Free Volume Relation to Clay Interlayer Spacing. In binary PNC systems with PA-6[2] or PS[29] as a matrix, at constant clay content the interlayer spacing,

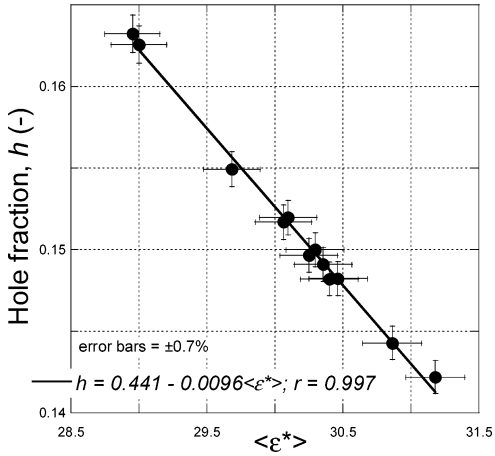

Figure 12. Hole fraction (at $P = 10$ MPa and $T = 500$ K) vs the experimental bulk-average energetic interaction parameter for all specimens in Table 2.

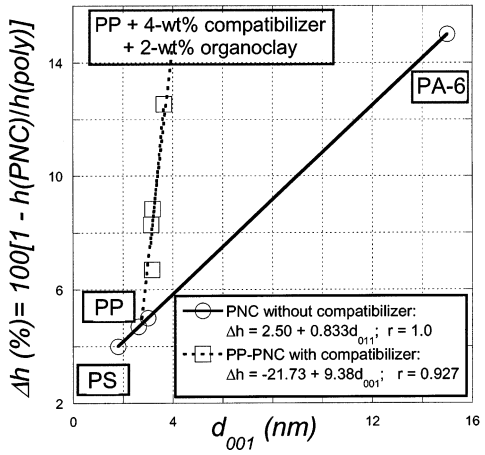

Figure 13. Correlation between the reduction of hole fraction and the interlayer spacing for the binary (circles: polymer + organoclay) and ternary (squares: PP-based PNC with a compatibilizer).

d_{001}, was found to correlate with the reduction of the hole fraction, Δh. These data (at the nominal loading of 2 wt % of organoclay) are replotted in Figure 13 along with the new values determined in the present studies. The d_{001} for the PP-based PNC was determined using wide-angle X-ray diffraction (XRD) within the angles $2\theta = 0.8°-10°$, using 0.01° step every 2 s. Two straight-line dependencies were obtained: (1) for binary systems: polymer + organoclay; (2) for ternary systems: PP + C15 + compatibilizer. Noteworthy is the high value of the correlation coefficient, $r = 1.000$ and 0.927 for the dependence (1) and (2), respectively. The (not shown) data for the higher concentration PNC's (4 wt % C15 + 8 wt % compatibilizer) scattered around the dependence (2). The observed correlations $\Delta h = \Delta h(d_{001})$ are unexpected, since Δh is determined in the molten state, whereas d_{001} is measured in solidified amorphous or semicrystalline specimens.

PNC Mechanical Properties. After observing correlations between the bulk-averaged interaction parameters, $\langle \epsilon^* \rangle$ vs $\langle v^* \rangle$, between $\langle \epsilon^* \rangle$ and the hole fraction, and between hole fraction and d_{001}, it was tempting to examine other potential relationships, e.g., between the eos parameters (or hole fraction) and the mechanical parameters of the PP-based PNC.

The specimens belonging to the four series of PP-based PNC (e.g., see Table 4) were injection-molded and

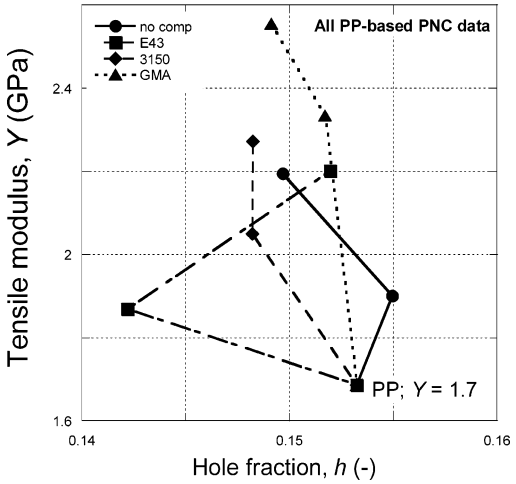

Figure 14. Correlation between tensile (Young's) modulus and hole fraction for the four series of PP-based PNC's. See text.

then tested according to ASTM in tensional, flexural, and impact (Izod) deformation.[43] Examples of the observed dependencies are shown in Figure 14, where the tensile modulus is plotted as a function of the hole fraction (n.b., proportional to d_{001}). The common point is for the neat PP matrix; the lines connect it with data first for PP + 2 wt % C15 + 4 wt % compatibilizer and then for PP + 4 wt % C15 + 8 wt % compatibilizer. Considering that the standard deviation for Δh is ±0.5% (or ±0.001 units) and the modulus ±5% (or ±100 MPa), there is no common tendency. Even more scatter was observed in a plot of the impact strength vs Δh (not shown). Clearly, in these complex systems the mechanical properties depend not only on the free volume and the interlayer spacing but also on other variables.

The mechanical performance of composites with crystalline matrix is difficult to predict because of the complex morphology. The crystallinity depends not only on the rate of cooling and nucleation by additives and contaminants but also on the processing history including shearing and residual stresses.[44] Furthermore, in the systems comprising a compatibilizer there are problems associated with the phase separation in polymer blends. In PO alloys the miscibility originates from small configurational entropy effects.[45] However, small differences in the macromolecular chain composition and/or configuration readily lead to immiscibility. For PP-based, compatibilized PNC, immiscibility was observed when the acid value of PP-MA was high, e.g., $A\# = 52$ mg of KOH/g, and the ratio of compatibilizer to organoclay low, viz. 1:1. Miscibility was recovered in PNC where the ratio was 3:1.

Within the four series of PNC compositions the one compatibilized with Epolene-43 showed a tendency for phase separation. The resin has a high acid value, $A\# = 47$ mg of KOH/g, low molecular weight ($M_w = 9.1$ kg/mol), and a high level of contamination (after purification the MAH content dropped from 9.79 to 3.81%). The PP/E43 binary blends phase-separated at E43 content of about 6 wt %. Observations under optical microscope showed a macroscale phase-separated blend of PP with 10 wt % Epolene-43 (see Figure 15).

As evident from the data in Figure 13, addition of 2 wt % of C15 and 4 wt % E43 efficiently reduced the hole fraction and increased the interlayer spacing to the highest value observed for this series, $d_{001} = 3.65$ nm.

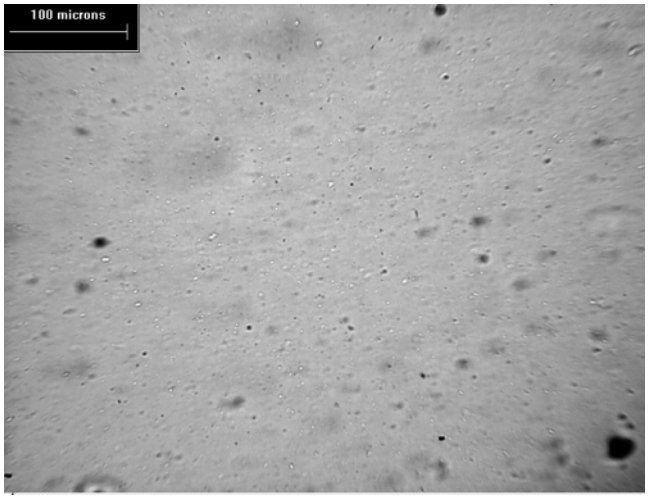

Figure 15. Blend of PP with 10 wt % of Epolene-43 in polarized light at $T = 190$ °C. The blend was prepared in a microextruder at $T = 180$ °C with $N = 100$ rpm and then transferred to hot stage microscope. Uniform dispersion of ca. 3.5 μm diameter drops was observed throughout the thickness.[46]

However, when the concentration was doubled, the hole fraction increased virtually to the level similar to that found for the PP matrix, while the interlayer spacing remained unaffected. The absence of a d_{001} change is understandable since in the studied PNC's the ratio of C15 to compatibilizer was kept constant at 1:2. Apparently, in these systems, the diffusion of homopolymer hardly contributes to the expansion of interlamellar galleries—the interlayer spacing depends on the reactive components in the system: intercalant and compatibilizer. The source of the abrupt increase of the hole fraction at 8 wt % E43 loading is most likely due to the phase separation and hence formation of the interphase. The viscosity of the interphase in the noncompatibilized polymer blends is known to be orders of magnitude lower than that of the two molten polymers[47]—low viscosity may be taken as a sign of high segmental mobility and thus increased free volume.

Evidently, the optical microscope is a poor tool for detecting phase separation. The domains must be large enough and have optical contrast in the molten state. Furthermore, the presence of organoclay may hinder coalescence, resulting in stabilized, fine droplets emulsion,[48] which would be difficult to see. The phase separation was not detected in other samples listed in Table 2.

VII. Summary and Conclusions

1. As previously observed for the poly-ϵ-caprolactam/clay system, we find that the Simha−Somcynsky (S−S) lattice−hole theory provides a good description of the *PVT* behavior of PP-based, clay-reinforced nanocomposites (PNC). Fitting the data to S−S equation of state gave the correlation coefficient, $r^2 \geq 0.999\,996$, and standard deviation of data, $\sigma < 0.0026$ mL/g.

2. Addition of ca. 2 wt % of organoclay to PP reduces the free volume function h by about 5% (at $P = 10$ MPa and $T = 500$ K). This compares with a considerably larger reduction of 12−16% over a range of T and P at 2 wt % organoclay loading, reported for PNC's based on PA-6. The smallest reduction of the matrix free volume (by about 4%) was observed for PS-based nanocomposites. There is a linear dependence of the reduction of the matrix polymer free volume function, Δh, and the interlayer spacing, d_{001}, at constant organoclay content.

3. Progressive clay exfoliation increases the surface area, capable to adsorb, and solidify growing amounts of organic species. Once more we emphasize the significance of the free volume function extracted from *PVT* measurements as a key element in the interpretation of PNC behavior. The clay surface area depends on the interlayer spacing and in turn determines matrix mobility.

4. In the quantitative evaluation of the "hairy clay platelet" (HCP) we have allowed for an exponential variation of matrix properties with orthogonal distance from the clay surface from a solidlike domain to a limit of neat polymer characteristics. The model is consistent with the significant reduction of the free volume in molten PNC. These systems are viewed as a suspension of solid particles in the matrix of polymer whose mobility depends on composition. Thus, the HCP is a clay platelet covered by a 6 nm thick layer of solidlike matrix and surrounding nimbus of macromolecules having mobility that increases with orthogonal distance from the clay surface for up to ca. 100 to 120 nm. Above this limit, neat matrix properties are expected.

5. While for binary system (polymer + organoclay) the dependence $\Delta h = \Delta h(d_{001})$ is common for all three so far tested nanocomposites, that for a ternary system (polymer + organoclay + compatibilizer) is different. Apparently, incorporation of the latter increases Δh with little if any effect on the interlayer spacing.

6. The plot $\Delta h = \Delta h(d_{001})$ may be used for evaluating different compatibilizing strategies—the closer the dependence for ternary systems is to that of binary ones the better.

7. For the investigated PP-based nanocomposites good consistency between the S−S eos parameters, between these and the hole fraction, and between hole fraction and interlayer spacing was obtained. By contrast, these measures correlated poorly with the mechanical properties in tension, flexion, or impact. This observation is particularly true for the three-component systems, in which addition of a compatibilizer may affect crystallinity, toughness, compositional homogeneity, etc.

Acknowledgment. Special thanks are due to members of the Polymer Composites team that prepared the samples (T.-M. Ton-That and Y. Simard), characterized these (F. Perrin-Sarazin, M. Sepehr, M. Plourde), and measured the *PVT* behavior (G. Chouinard).

References and Notes

(1) Rodgers, P. A. *J. Appl. Polym. Sci.* **1993**, *50*, 1061−1080.
(2) Simha, R.; Utracki, L. A.; Garcia-Rejon, A. *Composite Interfaces* **2001**, *8*, 345−353. Utracki, L. A.; Simha, R.; Garcia-Rejon, A. *Macromolecules* **2003**, *36*, 2114−2121.
(3) Simha, R.; Somcynsky, T. *Macromolecules* **1969**, *2*, 342−350.
(4) Utracki, L. A. *Clay-Containing Polymeric Nanocomposites*; Monograph 782 p; RAPRA: Shrewsbury, 2004.
(5) Jain, R. K.; Simha, R. *Macromolecules* **1980**, *13*, 1501−1508.
(6) Utracki, L. A.; Simha, R. *Macromol. Chem. Phys.*, *Mol. Theory Simul.* **2001**, *10*, 17−24.
(7) Israelachvili, J. N.; Tirrell, M.; Klein, J.; Almog, Y. *Macromolecules* **1984**, *17*, 204−209.
(8) Horn, R. G.; Israelachvili, J. N. *Macromolecules* **1988**, *21*, 2836−2841.
(9) Luengo, G.; Schmitt, F.-J.; Hill, R.; Israelachvili, J. N. *Macromolecules* **1997**, *30*, 2482−2494.
(10) Hentschke, R. *Macromol. Theory Simul.* **1997**, *6*, 287−316.

(11) Vacatello, M. *Macromol Theory Simul.* **2004**, *13*, 30−35 and references cited therein.
(12) Tanaka, G.; Goettler, L. A. *Polymer* **2002**, *43*, 541−553.
(13) Utracki, L. A. *Commercial Polymer Blends*, Chapman & Hill: London, 1998.
(14) Wang, Z. M.; Nakajima, H.; Manias, E.;Chung, T. C. *Macromolecules* **2003**, *36*, 8919−8922.
(15) Usuki, A.; Kato, M.; Okada,A.; Karauchi, T. *J. Appl. Polym. Sci.* **1997**, *63*, 137−139.
(16) Kato, M.; Usuki, A.; Okada, A. *J. Appl. Polym. Sci.* **1997**, *66*, 1781−1785.
(17) Kawasumi, M.; Hasegawa, N.; Kato, M.; Usuki, A.; Okada, A. *Macromolecules* **1997**, *30*, 6333−6338.
(18) Hasegawa, N.; Kawasumi, M.; Kato, M.; Usuki, A.; Okada, A. *J. Appl. Polym. Sci.* **1998**, *67*, 87−92.
(19) Hasegawa, N.; Usuki, A. *J. Appl. Polym. Sci.* **2004**, *93*, 464−470.
(20) Xie, W.; Gao, Z.; Pan, W.-P.; Vaia, R.; Hunter, D.; Singh, A. *ACS Polym. Mater. Sci. Eng. Proc.* **2000**, *82*, 284−285.
(21) Xie, W.; Gao, Z.; Pan, W.-P.; Hunter, D.; Singh, A.; Vaia, R. *Chem. Mater.* **2001**, *13*, 2979−2990.
(22) Xie, W.; Pan, W.-P.; Hunter, D.; Koene, B.; Tan, L.-S.; Vaia, R. *Chem. Mater.* **2002**, *14*, 4837−4845.
(23) Wang, D.-Y.; Parlow, D.; Yao, Q.; Wilkie, C. A. *J. Vinyl Add. Technol.* **2001**, *7*, 203−213.
(24) Wang, D.-Y.; Wilkie, C. A. *Polym. Degrad. Stab.* **2003**, *80*, 171−182.
(25) Du, J.-X.; Zhu, J.; Wilkie, C. A.; Wang, J.-Q. *Polym. Degrad. Stab.* **2002**, *77*, 377−381.
(26) Zhu, J.; Start, P.; Mauritz, K. A.; Wilkie, C. A *Polym. Degrad. Stab.* **2002**, *77*, 253−258.
(27) Zhang, J.; Wilkie, C. A. *Polym. Degrad. Stab.* **2003**, *80*, 163−169.
(28) Newman, A. C. D., Ed.; *Chemistry of Clays and Clays Minerals*, Mineralogical Society Monograph No. 6; Longman Scientific & Technical: Burnt Mill, Harlow, Essex, 1987.
(29) Tanoue, S.; Utracki, L. A.; Garcia-Rejon, A.; Tatibouët, J.; Cole, K. C.; Kamal, M. R. *Polym. Eng. Sci.* **2004**, *44*, 1046−1060.
(30) Oya, A.; Kurokawa, Y. *J. Mater. Sci.* **2000**, *35*, 1045−1050.
(31) Lee, J.-W.; Lim, Y.-T.; Park, O.-Ok *Polym. Bull. (Berlin)* **2000**, *45*, 191−198.
(32) Morgan, A. B.; Harris, J. D. *Polymer* **2003**, *44*, 2313−2320.
(33) Boucard, S.; Duchet, J.; Gérard, J. F.; Prele, P.; Gonzalez, S. *Macromol. Symp.* **2003**, *194*, 241−246.
(34) Ton-That, M.-T.; Perrin-Sarzin, F.; Bureau, M.; Cole, K. C.; Denault, J. *SPE Tech. Pap.* **2004**, *67*, 1523−1527.
(35) Ton-That, M.-T.; Cole, K. C.; Denault, J.; Perrin, F. *SAMPE Tech. Conf. Seattle, WA* **2001**, *33*, 720−727.
(36) Ton-That, M.-T.; Cole, K.; Denault, J.; Bureau, M. *4th Canadian International Composites Conference*, Ottawa ON, Canada, Aug 19−22, 2003 (CANCOM 2003).
(37) Roux, C.; Huneault, M. A.; Champagne, M. F. *SPE ANTEC.* **1998**, *44*, 2−6.
(38) Zoller, P.; Walsh, D. *Standard Pressure−Volume−Temperature Data for Polymers*; Technomic: Lancaster, 1995.
(39) Hu, H.-W.; Granick, S. *Science* **1992**, *258*, 1339−1342.
(40) Hentschke, R. *Macromol. Theory Simul.* **1997**, *6*, 287−316.
(41) Utracki, L. A.; Lyngaae-Jørgensen, J. *Rheol. Acta* **2002**, *41*, 394−407.
(42) Utracki, L. A., unpublished data on PVT behavior of polystyrenes, 2001.
(43) Ton-That, M.-T., personal communication, 2004.
(44) Nowacki, R.; Monasse, B.; Piórkowska, E.; Gałęski, A.; Haudin, J. M. *Polymer* **2004**, *45*, 4877−4829.
(45) Utracki, L. A., Ed., *Polymer Blends Handbook*; Kluwer Academic Publishers: Dordrecht, 2002.
(46) Sepehr, M., personal communication, 2004.
(47) Lyngaae-Jørgensen, J.; Thomsen, L. D.; Rasmussen, K.; Sondergaard, K.; Andersen, F. E. *Int. Polym. Process.* **1988**, *2*, 123−130.
(48) Ray, S. S.; Pouliot, S.; Bousmina, M.; Utracki, L. A. *Polymer*, in press.

MA048262Z